Article Title

The Möbius Phenomenon in Generalized Möbius–Listing Bodies With Cross Sections of Odd and Even Polygons

Authors

J. Gielis, I. Tavkhelidze

Corresponding Author

J. Gielis – johan.gielis@uantwerpen.be

Research Article

The Möbius Phenomenon in Generalized Möbius-Listing Bodies with Cross Sections of Odd and Even Polygons

J. Gielis[1,*] iD, I. Tavkhelidze[2]

[1]*Department of Biosciences Engineering, University of Antwerp, Belgium*
[2]*Faculty of Exact and Natural Sciences, Tbilisi State University, University Street 13, Tbilisi 0186, Georgia*

ARTICLE INFO

ABSTRACT

In the study of cutting Generalized Möbius-Listing bodies with polygons as cross section, it is well known that the Möbius phenomenon, whereby the cutting process yields only one body, occurs only in even polygons with an even number of vertices and sides, and only in the specific when the knife cuts through the center of the polygon. This knife cuts from vertex to vertex, vertex to side or side to side, cutting exactly two points on the boundary of the polygon. This is called a chordal knife, in connection to the chord cutting a circle. If the knife is a radial knife, i.e. it cuts only one point of the boundary, the Möbius phenomenon can occur both in odd and even polygons, but only when the radial knife cuts the center of the polygon. One finding is the reduction of a problem in 3D (with internal geometry) to a planar problem and the concomitant reduction of the analytic representation with multiple parameters to a few only. The shape of the cross section and number of twisting in the 3D representation suffice and reduce the problem to cutting of regular polygons and cyclic permutations.

1. INTRODUCTION

1.1. Generalized Möbius-Listing Bodies and Surfaces

Möbius bands are icons of mathematics, defined by a line swept along a circular path, but with a twist of 180° before connecting with the original line. Generalized Möbius-Listing GML_m^n surfaces and bodies are a generalization of Möbius bands and the Möbius phenomenon of one sided surfaces [1]. Generalized Möbius-Listing GML_m^n surfaces and bodies are toroidal structures obtained from cylinders whose cross sections have rotational symmetry, e.g. regular polygons, and with the centers of all cross sections forming the basic line of the cylinder (Figure 1 left). The toroidal structure results from joining the two ends of the cylinder after n twists of the cylinder around the basic line, with both m and n positive integers.

GML_m^n bodies and surfaces are closed toroidal structures but are a subset of Generalized Twisting and Rotating bodies GTR_m^n bodies and surfaces.

Definition 1: Generalized twisting and rotating bodies GTR_m^n bodies and surfaces are defined by (1):

$$
\begin{aligned}
X(\tau, \psi, \theta, t) &= T_1(t) + [R(\psi, \theta, t) + p(\tau, \psi, \theta, t) \\
&\quad \cos(\psi + \mu g(\theta)] \cos(\theta + M(t)) \\
Y(\tau, \psi, \theta, t) &= T_2(t) + [R(\psi, \theta, t) + p(\tau, \psi, \theta, t) \\
&\quad \cos(\psi + \mu g(\theta)] \sin(\theta + M(t)) \\
Z(\tau, \psi, \theta, t) &= T_3(t) + Q(\theta, t) + p(\tau, \psi, \theta, t) \sin(\psi + \mu g(\theta))
\end{aligned} \tag{1}
$$

X, Y, Z, t is the ordinary notation for space and time coordinates and τ, ψ, θ are local coordinates where $\tau \in [-\tau^*, \tau^*]$, with $0 < \tau$; $\psi \in [0; 2\pi]$ and $\vartheta \in [0; 2\pi h]$, with $h \in \mathbb{R}$.

The functions $T_{1,2,3}(t)$, $R(\psi, \theta, t)$, $p(\tau, \psi, \theta, t)$, $M(t)$ and $Q(\theta, t)$, as well as parameter μ (defining twisting around the basic line), define simple movements. With these analytic representations complex movements can be studied and decomposed into simple movements; this line of research goes back to Gaspar Monge [2].

Definition 2: Generalized Möbius-Listing bodies GML_m^n are defined by (2) and (3):

$$
\begin{cases}
X(\tau, \psi, \theta) = \left(R(\theta) + p(\tau, \psi) \cos\left(\dfrac{n\theta}{m}\right) - q(\tau, \psi) \sin\left(\dfrac{n\theta}{m}\right) \right) \cos(\theta) \\
Y(\tau, \psi, \theta) = \left(R(\theta) + p(\tau, \psi) \cos\left(\dfrac{n\theta}{m}\right) - q(\tau, \psi) \sin\left(\dfrac{n\theta}{m}\right) \right) \sin(\theta) \\
Z(\tau, \psi, \theta) = K(\theta) + \left(p(\tau, \psi) \sin\left(\dfrac{n\theta}{m}\right) + q(\tau, \psi) \cos\left(\dfrac{n\theta}{m}\right) \right)
\end{cases} \tag{2}
$$

or, alternatively,

Corresponding author. Email: johan.gielis@uantwerpen.be
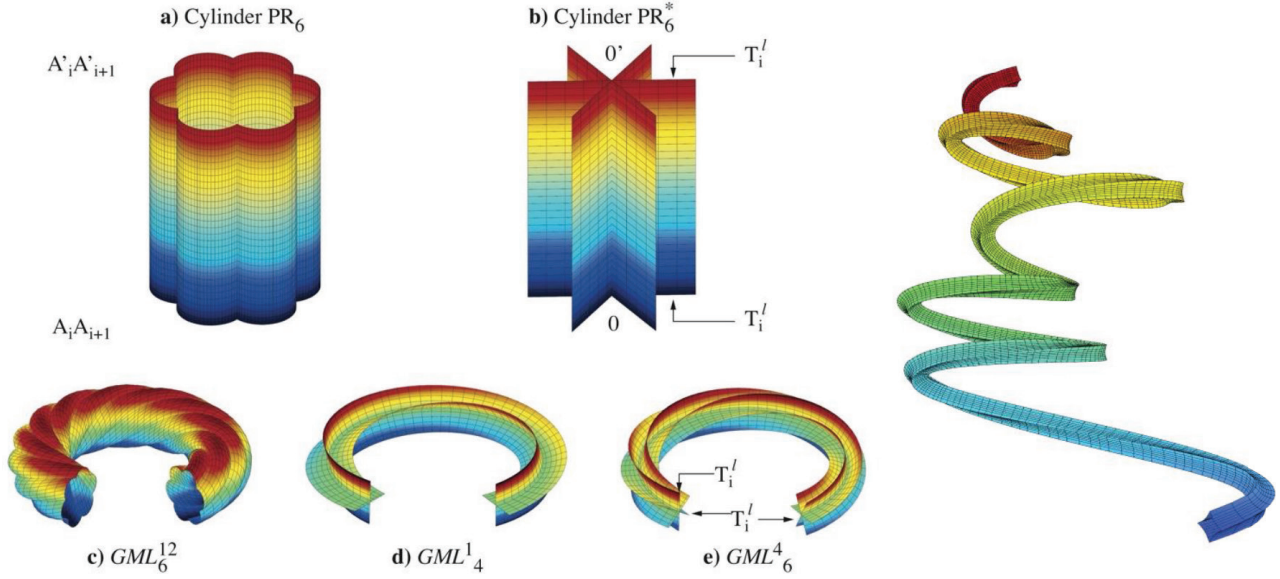
Figure 1 | Left: Identification of vertices $A_i^{'}$ or $T_i^{'}$, with twists leading to torus GML_m^n. Right: GTR body.

$$\begin{cases} X(\tau, \psi, \theta) = \left(R(\theta) + p(\tau, \psi)\cos\left(\psi + \frac{n\theta}{m} \right) \right)\cos(\theta) \\ Y(\tau, \psi, \theta) = \left(R(\theta) + p(\tau, \psi)\cos\left(\psi + \frac{n\theta}{m} \right) \right)\sin(\theta) \\ Z(\tau, \psi, \theta) = K(\theta) + p(\tau, \psi)\sin\left(\psi + \frac{n\theta}{m} \right) \end{cases} \quad (3)$$

In the notation GML_m^n, m relates to the symmetry of the cross section, and n to the number of twists relative to m. The choice of regular polygons and of straight knives can be generalized to any convex or concave m-symmetrical cross section. For the functions $R(\theta)$ and $p(\tau, \psi)$ (path and cross section of the GML_m^n, respectively) Gielis transformations defined by (4) can be used [2–8]. They provide for a unifying description for a wide range of natural and abstract shapes, including regular polygons [9,10]:

$$\rho(\vartheta; A, B, m, n_1, n_2, n_3) =$$
$$\frac{1}{\sqrt[n_1]{\left| \frac{1}{A}\cos\left(\frac{m}{4}\vartheta \right) \right|^{n_2} \pm \left| \frac{1}{B}\sin\left(\frac{m}{4}\vartheta \right) \right|^{n_3}}} \cdot f(\vartheta) \quad (4)$$

The advantage of these analytic representation is the knowledge of the domain using a limited set of parameters to describe complex movements [2]. Furthermore, a wide variety of classical problems in topology, based on algorithmic approaches (e.g. folding and gluing) can now be studied using analytic geometry. Indeed, these analytic representations or equations substitute for recipes or algorithms to generate Möbius strips, tori, Klein bottles, canal surfaces or more complex shapes, or recipes for studying combinatorial problems, especially when these domains have internal symmetry whereby differentiated zones and sectors result when GML_m^n surfaces or bodies are cut.

1.2. Cutting of Möbius-Listing Bodies and the Reduction to a Planar Problem

In case the cylinder is a strip and it is given a half twist (180°) before joining, the classic Möbius band results, a GML_2^1 surface. The half twist for $\frac{m}{2} = n = 1$. The results of cutting GML_2^n surfaces based on a strip, have been classified in full generality for any integer value of n (for all multiples of n or 180°), for all cutting lines or strips (containing the basic line or not) of and for any number of cuttings [1]. Results have been reported for cutting GML with particular symmetries [2–7] and the general case was solved in Gielis and Tavkhelidze [8].

Definition 3: Cutting is performed with (1) a straight knife, which (2) cuts perpendicular to the polygonal cross section of the GML_m^n surfaces and bodies, and (3) the knife cuts the m-polygon boundary exactly in two points or two times (depending on the thickness of the knife). For (3) there are three possibilities: the cut of the polygon can be from a vertex to a vertex VV, from a vertex to a side or edge VS, or from side to side SS (=edge to edge). The precise orientation of this knife (and the positions where it cuts the boundary) is maintained during the complete cutting process, until the knife returns to its starting position, and the cutting is completed. The point of the knife traces out a toroidal line along the GML_m^n body or surface.

Depending on the number of twists, a number of independent bodies results, that is related to the divisors of m. Cutting of GML_m^n surfaces and bodies along the toroidal structure has unveiled a close link with the study of knots and links, and with the coloring of surfaces. Figure 2 gives one example of a SS-cut in a pentagon. Table 1 in Supplementary information gives the results for cutting GML_4^n and GML_5^n for different values of n.

Alternatively, one can also fix the knife and move the GML_m^n surface or body through the knife. The cutting process of the three

dimensional GML_m^n bodies can then be related one-to-one to plane geometry, and the 3D problem becomes a planar one. Now, the d_m knife is a line of infinite length (1), rotated m times or a divisor thereof.

Definition 4: The analytic definition of d-knife (1) is a construction with straight lines, whereby the number of straight lines is either m or one of its divisors:

$$\sin\left(\alpha + \frac{2\pi}{m}i\right)x_i + \cos\left(\alpha + \frac{2\pi}{m}i\right)y_i + \delta = 0,$$

$$i = 0, 1, ..., m-1; \; -\frac{\pi}{m} \le \alpha \le \frac{\pi}{m}, \tag{5}$$

with α the rotation parameter, and δ the translation parameter of this infinite line [8,11,12].

Indeed, with the analytical definition of the geometrical d_m knife [11] all possible cuttings of regular polygons can be studied with the number of blades on the knife either m or a divisor of m. This d_m knife with m blades cuts from vertex to vertex, vertex to side or side to side, with each blade cutting exactly two points on the boundary of the polygon.

In the case $m = 8$ the $d_m = m$ knife has 8 blades, but for the octagon one can also have one-bladed, two-bladed and four-bladed knives. In Figure 3 the results of cutting an octagon with the $d_{m=8}$ knife with eight blades are shown. In the left figure one observes that d_m cuts from vertex to the opposite vertex, but the analytical definition of the knife allows for a rotation resulting in the side to side cuts in Figure 3 (right). A translation or a combination of translation and rotation, resulting in vertex-to-vertex, vertex-to-side and side-to-side cuts is also possible (Figure 3, all other figures). This d_m knife can cut from vertex to vertex, vertex to side or side to side, cutting exactly two points on the boundary of the polygon, and if m is an even number, then always some values of n exist for the Möbius phenomenon of the strip is realized.

Remark 1: It is noted that in the case $m = 8$ and the knife passing through the centre one counts only four chordal knives, but that is because the chordal knives overlap two by two.

The Annex in Gielis and Tavkhelidze [8] shows all possible cuts for $m = 6,…,10$. These methods are intimately linked to combinatorial problems, for example the Euler problems of drawing non-dissecting diagonals in polygons. Another combinatorial problem is the number of intersections of diagonals in the interior of regular n-gon (OEIS A006561 [13]). In the three left figures of Figure 3 the process of cutting from vertex to vertex is shown for an octagon. When these three figures are combined, one can compute the number of intersections of diagonals in the interior of regular n-gon (OEIS A006561 [13]). Indeed, Figure 3 is a dissection of this problem for the octagon into three, namely cuts with chordal d_m knife from $V_1 \rightarrow V_5$ from $V_1 \rightarrow V_4$ and from $V_1 \rightarrow V_3$, using the analytic definition of knives (5), and rotation and translation of the knife. Diagonal cutting problems are vertex to vertex, but our methods can also handle VS and SS cuttings or drawing lines.

1.3. The Occurrence of the Möbius Phenomenon

It is noted that the solution of the problem by a reduction of dimensions, is also reflected in the reduction of parameters in the analytic expressions: only the cross section $p(\tau, \psi)$ and the twisting parameter n, are involved. With this reduction it was found that the Möbius phenomenon, whereby the cutting process yields only a single and "one-sided" body, similar to the original Möbius strip or ribbon, occurs only in even polygons with an even number of vertices and sides and only in the specific case when the knife cuts through the center of the polygon (Figure 3 left and right).

This means that after a full cutting of the GML_m^n body, only one body results, which displays the Möbius phenomenon of one-sided
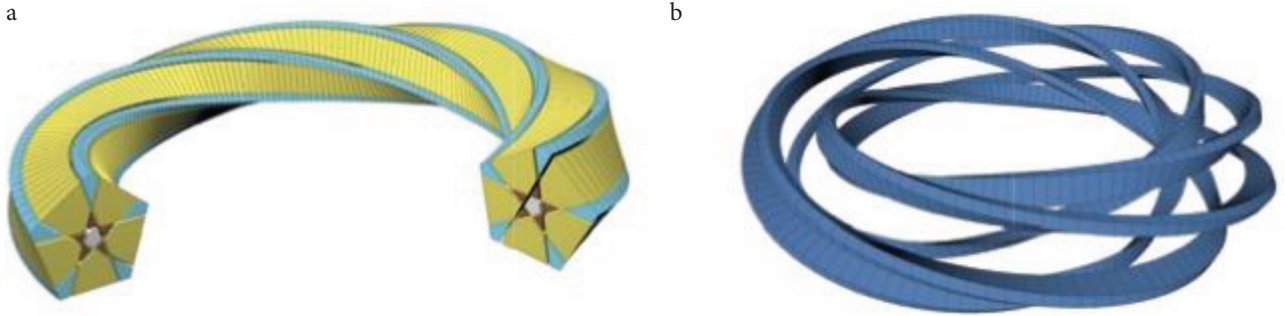
Figure 2 | (a) A pentagonal GML_5^n body with four different bodies after cutting, each body indicated by a different color. (b) One of the resulting structures after cutting, forming a Link-4 structure with the three other resulting bodies.
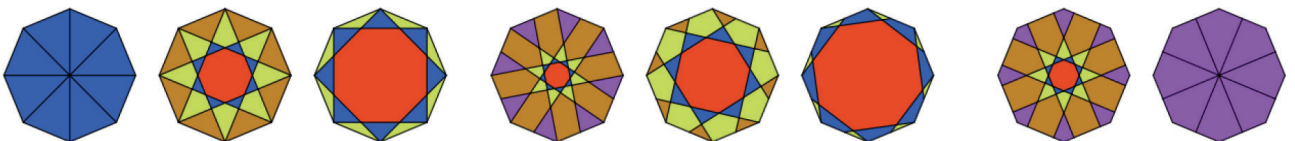
Figure 3 | Cutting and octagon with d_m knife.

bodies (in Figure 3, different colors in one shape indicate different bodies after cutting, so in the figures left and right we only have one body). In the case of GML_m^n surfaces, this cutting results in 1 ribbon which is one sided, and in the case of GML_m^n bodies this results in one single body displaying the Möbius phenomenon. In the case of GML_8^n bodies for example, depending on how the cut is made, such bodies can be triangular (Figure 3 left) or quadrangular (kite-shaped; Figure 3 right).

Remark 2: In a classical Möbius band an arrow moving along the ribbon is reversed after one full rotation, and two rotations are necessary for the arrow to coincide with the original one. The phenomenon after one rotation is often referred to as non-orientability. In terms of visualization: if one travels on one particular trajectory of such one-sided ribbons resulting from cutting GML_m^n surfaces, this is similar to travelling along the classic Möbius strip. In the case of GML_m^n bodies with Möbius phenomenon after cutting, travelling along each of the sides of the triangular bodies is similar to traveling along the classic Möbius band.
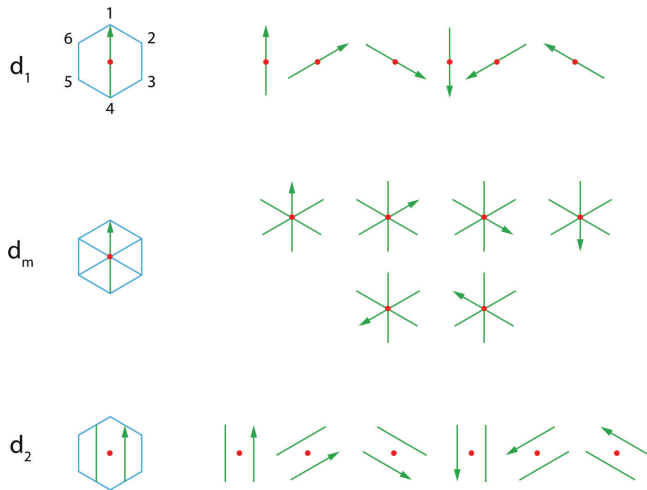
For the necessary conditions for obtaining the Möbius phenomenon after cutting GML_m^n surfaces or bodies, we have the following:

1. The number m has to be even ($m = 2, 4, 6, …$). The Möbius phenomenon never occurs when the polygon has an odd number of vertices and sides [6–8].

2. The knife has m blades cutting all vertices with maximal length of the knife (i.e. from one vertex or side to the opposite one, then repeating this for every vertex).

3. The d_m knife has to cut through the center (cuts are either vertex to opposite vertex, or side to side through the center of the polygon).

In investigating the conditions under which the Möbius phenomenon could also occur when m is an odd number ($m = 3, 5, 7, …$), we prove the following:

Proposition 1: If the knife is a radial knife the Möbius phenomenon can occur both in odd and even polygons.

2. FROM CHORDAL TO RADIAL KNIVES

For a hexagon (Figure 4), one can visualize the m knives and their rotation for a d_1 knife cutting from vertex 1 to 4 and for d_m knife for all vertices. A translated knife is shown for d_2. The rotated knives on the right show the orientation of the knife for every case when it cuts GML_m^n bodies or surfaces, with $n = m$ twists. The point of the arrow coincides with the toroidal lines on the twisted GML_m^n bodies or surfaces every 60°. The original d_m knife is called a chordal knife, in connection to the chord cutting a circle. The symbol d refers to diagonal cutting of polygons, but chordal or d_m knife is more general and is related directly to the classical trigonometric functions. A chord divides a circle (or polygon) into two distinct pieces and defines the sine function (the chord is $2 \sin \alpha$, or AB in Figure 5a), and by virtue of the Pythagorean theorem also the cosine function (OC).

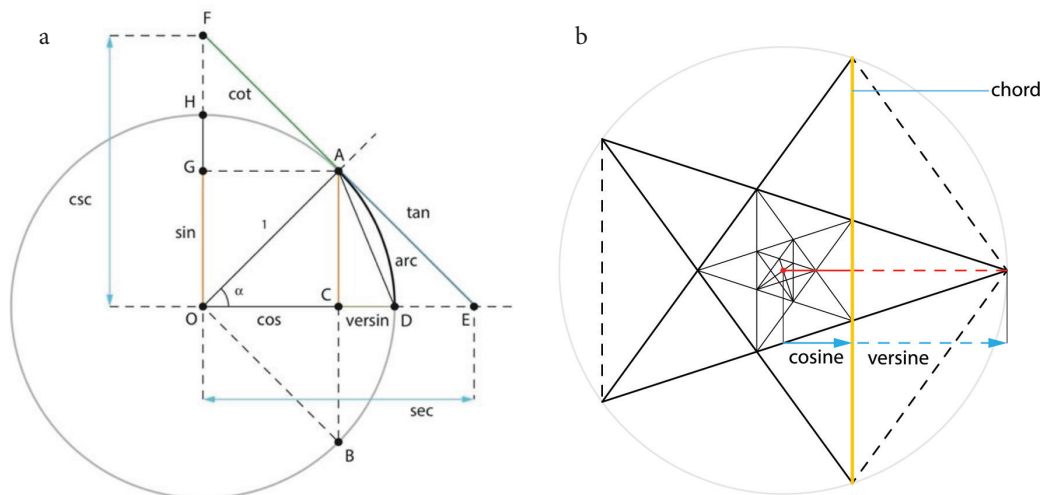**Figure 4** | Chordal knife with 1, 2 and 6 blades.

Figure 5 | (a) Classical trigonometric functions with the radius OA as radial knife and the line AB as chordal knife. (b) Rotating and zooming the yellow knife allows for the infinite scaling of the pentagon and pentagram.

In Figure 5a the line OF corresponds to half the knife d_1 in Figure 4. For this chordal knife in vertical direction and going through the center the chord is maximal; the sine equals 1 and the cosine equals zero. The line AB on the other hand corresponds to the translated knife in the case of knife d_2 in Figure 4.

In Figure 5b the relation of chords to polygons is shown, with the chord, the cosine/versine and sine/coversine as interesting functions for the pentagon. On a circle five equally spaced points represent the vertices of a pentagon, which is constructed by connecting vertex V_i with vertex V_{i+1}, then vertex V_{i+1} with vertex V_{i+2}, until one returns at vertex V_i. The pentagram is constructed by connecting vertex V_i with vertex V_{i+2} (Figure 5b).

In particular the adjacent chords of the pentagram (e.g. the yellow chord from V_1 to V_3 and the chord from V_3 to V_5) form two long and equal sides of a so-called golden triangle, an isosceles triangle with one angle $\dfrac{\pi}{5}$ and two angles of $\dfrac{2\pi}{5}$. Two non-consecutive sides of a pentagram (e.g. the chord from V_1 to V_3 and the chord from V_2 to V_4) divide each other in mean and extreme ratio. Such constructions are based on the classical compass and ruler construction, but polygons and polygrams can be constructed using d_m knives (5). In these cases, the knives do not cut but are simply drawing tools.

If we now limit the knife in (5) to the half line OF or OE originating in the origin or center of the polygon, we obtain a radial knife (Figure 6). The name derives from radius versus the diameter in chordal knives. It cuts the polygon boundary only in one point.

Remark 3: Chordal and radial knives can belong to four different classes:

d_{cc} chordal knife, through the center 0 (d_1 and d_m in Figure 4)

$d_{c\bar{c}}$ chordal knife, not through the center (d_2 in Figure 4)

d_{rc} radial knife originating at the center (d_1 in Figure 6)

$d_{r\bar{c}}$ radial knife not through the center

Remark 4: A radial cut d_{rc} is also a half-line or ray, corresponding to the classical position vector, the most elementary and natural geometric object. This half-line can be translated using δ or rotated using α, the translation and rotation parameters in (5), respectively. The d_{rc} or $d_{r\bar{c}}$ radial knives can also be moved via a combination of translation and rotation. The length of the d_{rc} is defined as the length from origin to the perimeter but can be extended or made shorter in the case of $d_{r\bar{c}}$ knives as long as the knife cuts only one point on the surface.

The $d_m = d_{cc}$ knives found their origin in cutting of bamboo culms lengthwise. Examples of both chordal and radial knives are found

in the art of wood sawing, where due to the nature of wood, saws are more efficient than knives (Figure 7). Plain sawing corresponds to using chordal saws, whereas for quarter and rift sawing, the saw is a radial saw, with d_{rc} in the case of rift sawing and $d_{r\bar{c}}$ in the case of quarter sawing.

3. USING RADIAL KNIVES FOR ODD AND EVEN POLYGONS

3.1. The Conditions for Odd

Now, for proving that the radial knife also works when m is an odd number, the strategy is to look only at the simplest possibility, which for m even is a cut through center or origin from a vertex to the opposite vertex, for all vertices (Figure 4 left and d_m in Figure 4). In this case the planar geometrical configuration is $m/2$. In 3D GML_m^n surfaces and bodies the Mobius phenomenon occurs when m is even and $n/2$. This is similar to the classic Möbius ribbon, which is a ribbon (a special case of a bilaterally symmetric shape with $m = 2$), twisted 180° before closing.

Because of the equivalence of the cutting of GML_m^n surfaces and bodies and their representations in plane geometry as in Figure 3, the Möbius condition is achieved when in planar view all diagonals are used, in other words, when $d_m = m$ (Figure 4). This can obviously
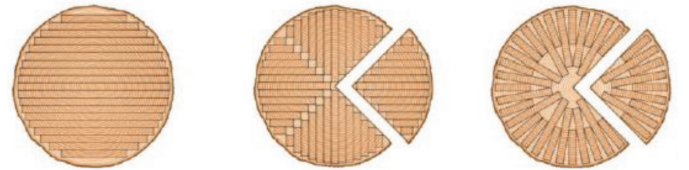
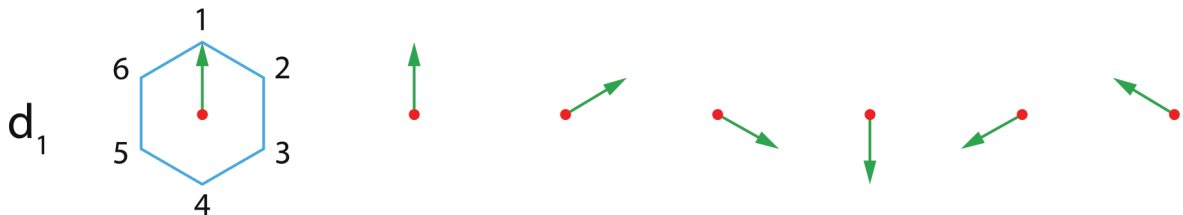**Figure 7** | Plain, quarter and rift sawing of logs.

Figure 6 | Left: d_{rc} radial knife originating at the center (d_1). The other rotated arrows indicated the position of the radial knife when traveling around a GML_6^6 in one rotation.

also be achieved with radial knives, for example using all orientations of d_1 knives in Figure 6.

It is then required to have the same situation in odd polygons. It is easy to see that this is very well possible with radial knives as shown in Figure 6, but five radial knives are needed or in general, an amount of m knives, in contrast to an amount of $m/2$ of chordal knives as in d_m in Figure 6. Generalizing radial knives d_{rc} for any symmetry, i.e. rotating the radial d_1 knife to m positions as in Figure 8, results in m radial knives for m-regular polygons, irrespective of whether m is even or odd. In 3D GML_m^n surfaces and bodies being cut with radial knives, this means that $n = m$ twists are needed to connect both ends of the cylinder. Then the full cutting results in a single one-sided body, displaying the Möbius phenomenon, as stated in Proposition 1.

3.2. Zones Created with Cutting

Using chordal knives in polygons results in different zones, the number and shapes of which are defined by the mode of cutting [12]. In Figure 3, some examples are shown for octagons. The different colors of the zones correspond to different bodies resulting from cutting GML_8^n bodies with octagonal cross sections. In the case of chordal knives going through the origin, the number of separate sectors is $2m$ in the case of regular polygons when m is odd (Figure 9a for $m = 9$) but the number of separate sectors is m in the case of m-regular polygons when m is even (Figure 9b for $m = 12$). A full classification has been reported in [9].

In the case of radial knives however, the number of sectors is m, irrespective whether m is even or odd. In Figure 10 this is shown for cutting of equiangular triangles, with chordal knives through the origin from vertex to side (Figure 10a) or from side to side (Figure 10c). The number of different chordal knives $m = 3$ results in $2m = 6$ sectors. If the cut is performed with three radial knives starting from the origin to vertex or two sides, one obtains exactly m sectors, for both odd and even polygons (Figure 10b and 10d). These sectors are a combination of one light blue and one dark blue sector in Figure 10.

This leads to three sectors which are congruent. Likewise, when the knives are rotated, always three congruent sectors are obtained. In the 3D GML_3^n bodies with $m = n$ twists, this results in one body after cutting, with Möbius phenomenon.

Congruence of sectors in the planar view is of primordial importance. These congruent sectors are independent of the number of cuts with the radial knife, but only in the case that the number of knives used is m, the Möbius phenomenon occurs. In other words, only in that case one body results after cutting the GML body. The

cross section of this single body is the same along the whole GML body, due to the congruence of shapes.

With the demonstration in 3D in Subsection 3.1 and the congruence of sectors in planar view, we then have [14]:

Theorem 1: If the knife cutting a GML_n^n body is a radial knife with origin in the center of the polygonal cross sections and cuts all sides of the polygon with equal spacing the Möbius phenomenon will occur in both in odd and even polygons.

4. RADIAL KNIVES AND LAMÉ'S SUPERCIRCLES

One constant result in the studies of cutting GML_m^n surfaces and bodies has been that a cutting resulting in only one body displaying the Möbius phenomenon, was limited to cases where m is an even number [5–7]. Using radial knives instead of chordal knives, it is shown that the Möbius phenomenon for GML_m^n bodies and surfaces can occur for m-regular polygons (or more generally with cross section with C_m rotational symmetry) when the knife crosses or originates in the center of the polygon. In the 2D planar representation, this means that all the sectors remain connected, like in the 3D GML_m^n. In this paper it was assumed that the cross section of the GML remains constant along the whole structure. In a forthcoming paper it is shown that the cross section can be variable along the GML using the analytic representation. In fact, it will be shown that only one cross section with rotational symmetrical shapes is enough to obtain the Möbius phenomenon.

A main strategy in our joint studies are the analytic representations. These are threefold: namely (1) the analytic representations of GML_m^n bodies and surfaces, (2) the extension with Gielis curves
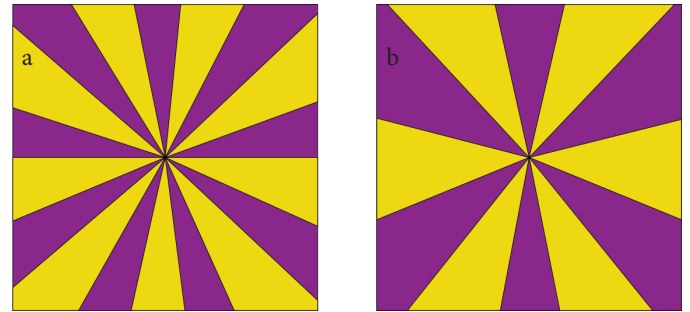
Figure 9 | Number of zones created with chordal knife with m blades through the origin and vertices for $m = 9$ (a) and $m = 12$ (b).
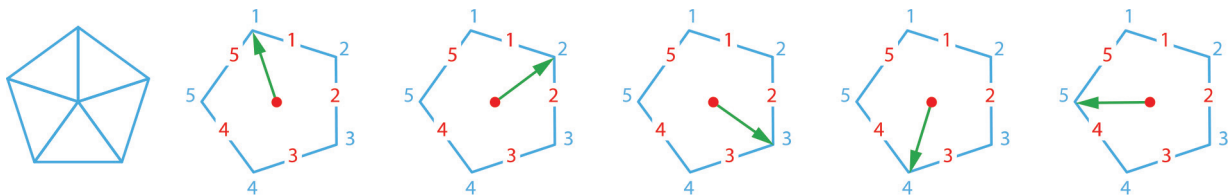
Figure 8 | Five radial knives in a pentagon.

and transformations for cross sections and basic lines, and (3) the geometrical representation of the knives used for the study of cutting GML_m^n [8].

First, classic Möbius ribbons or strips where generalized to GML_m^n bodies and surfaces, whereby the strip is a special case of GML_2^n surface. This led to a full classification of cutting results for GML_2^n [1,2], not only for line cuts, but also for slit cuts, cutting aways "zones". Results of cutting GML_m^n surfaces and bodies with rotational symmetry $C_m = 3, 4, 5, 6$ were also classified, and the general case was proven in Gielis and Tavkhelidze [8].

Second, the extension with Gielis transformations both for cross sections and the basic line of the toroidal structure, showed the generality of the results. They act as a transformation on curves or functions $f(\vartheta)$ and are a generalization of Gabriel Lamé's superellipses, defined by $\left|\dfrac{x}{A}\right|^n + \left|\dfrac{y}{B}\right|^n = R^n$ (6). To deal with different symmetries, the original expression was expressed in polar coordinates, and more degrees of freedom n_1, n_2, n_3 were added. The symmetry parameter m folds the classic Cartesian coordinate system with four quadrants or sectors in a polar coordinate systems with m sectors (Figure 11 show subcircles). Lamé's Superellipses are defined by (4) for n_1, n_2, $n_3 = n$; $m = 4$.

Expression (4) is a Pythagoras-compact expression, since for n_1, n_2, $n_3 = 2$; $A = B = 1$; $m = 4$. in (4), the circle results. Parameter m can be an integer, a rational or irrational number, and (4) can define the cross section or the path, or both. By considering (4) as inequality, any

point inside (and/or outside) the curve is defined precisely. Obviously, one can define shapes with boundary thickness (annuli or shells) in this way.

Remark 4: Any of the curves in Figure 12 may serve as boundaries or as knives [8]. Similary, straight lines in the Poincaré disk, the two-dimensional representation of the hyperbolic plane, can serve as knives.

Third, the results of cutting of GML_m^n bodies could be related one-to-one with planar geometry, which led to the solution of the general case [7], and of the occurrence of the Möbius phenomenon for any integer or rational rotational symmetry, using the analytical definition of the d_m knife (5) [8,11].

The results in this paper is that the same analytic representation of a d_m knife but restricted to a half line resulting in radial knives, can be used to extend the possibility of having a single body with Möbius phenomenon after cutting GML bodies, with cross section regular polygons with both even and odd rotational symmetry. In this case, bodies (or polygons) are cut, but beyond cutting radial knives can also divide the plane into m sectors (chordal or diagonal knives divide the plane into $m/2$ sectors). By adding a direction and a length to these radial knives, this results in vectors. In other words, the same analytical definition adapted for radial knives, can describe knives, lines to separate sectors, drawing tools (e.g. drawing diagonals in polygons) or vectors. If we would call the radial knife an r_m knife, it is clear that it is directly related to radial distances, but now with m copies of one knife, spaced equally around the origin.
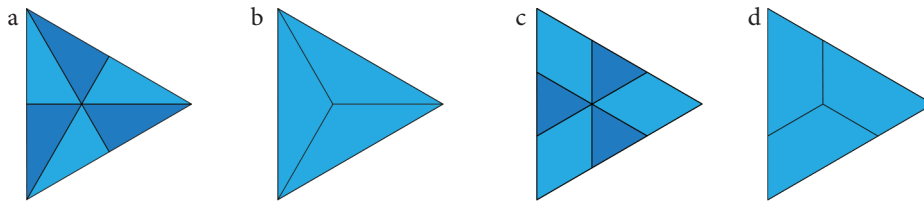
Figure 10 | Vertex to side and side to side cuts through the origin in a triangle, with chordal (a and c) or radial knives (b and d).
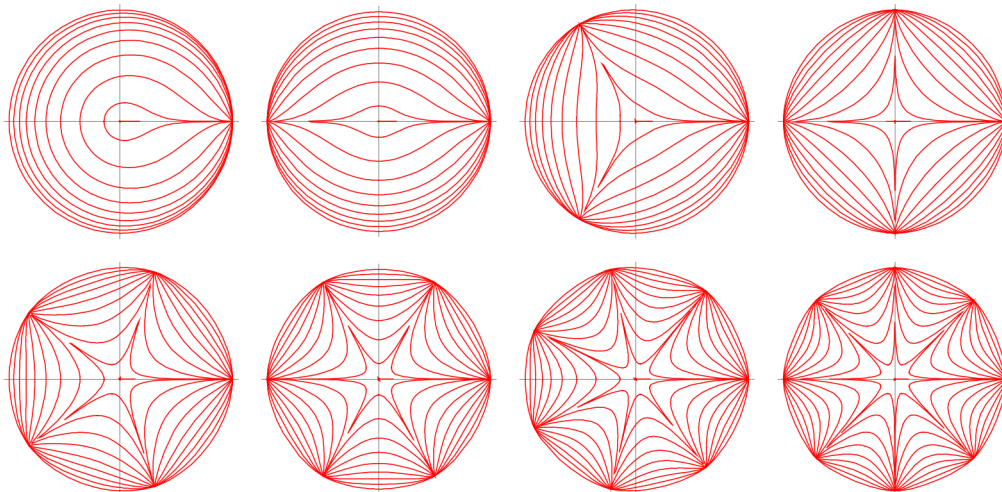
Figure 11 | Supercurves with all exponents n equal, but $m = 1, 2, …, 8$. All exponents $n_1 = n_2 = n_3 \leq 2$. Subcircles for $m = 4$, upper right.

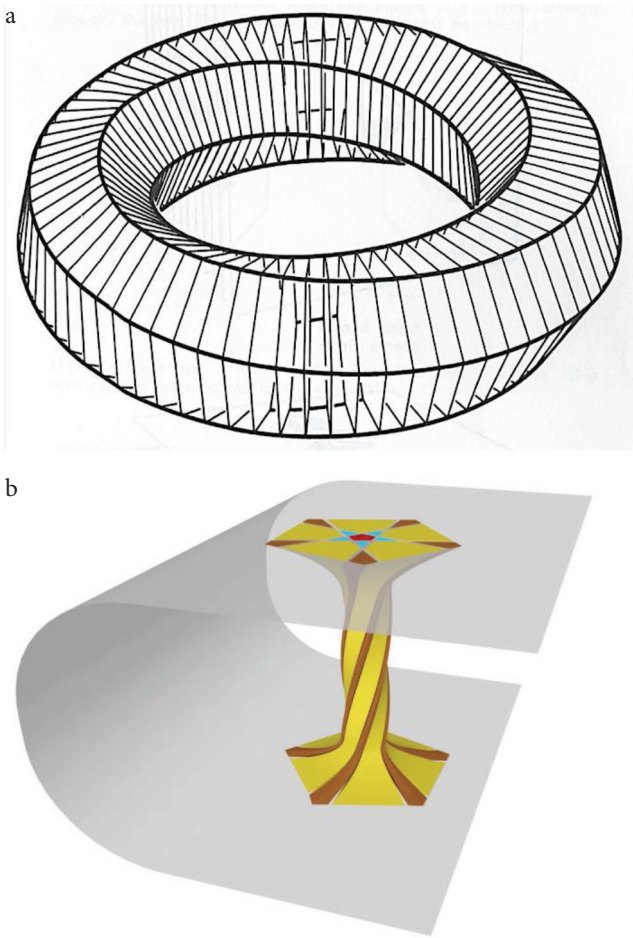**Figure 12** | The rope model of the helical heart.

Figure 13 | (a) GML_6^n Fibre bundle [17]; (b) A GML_5^n wormhole.

Finally, a beautiful consequence is that if one applies Lamé's idea of generalizing circles and ellipses into supercircles and superellipses defined in a Cartesian system with four quadrants, onto a plane divided into m sectors, one readily sees that the Gielis formula (4) is exactly doing the same as the knives: division of the plane into m sectors. To each of these sectors then Lamé's generalization of the Pythagorean Theorem can be applied. At the same time (4) adds more degrees of freedom and it is a continuous transformation. So we find a complete integration of Gielis Transformations and GML_m^n bodies and surfaces.

5. CONCLUSION AND FUTURE WORK

5.1. Biology, Physics and Geometry

The combination of chordal and radial knives and their analytic representation is directly related to classical trigonometric functions and the position vector. Because of the combination with Gielis transformations, it is expected that many of the phenomena described above, will find use in many fields of physics and biology [8].

One particular example of a shape that can directly be interpreted as a GML_m^n structure is the helical heart of animals, a structure discovered by the Spanish cardiologist Dr. Torrent-Guasp [15,16], described by a rope model. This is a GML_m^n structure of which the basic line is a half-angle defined by $m = 1/2$ in (4), closing after 720°. The rope model of the heart (Figure 12) shows the beginning and the end of the myocardial band at the aorta and pulmonary artery (right), the circumferential wrap of the basal loop (center) and the helix with basic line a half-angle $m = $ (left). This halfangle is directly related to the Möbius phenomenon.

It is remarkable that the connection of geometry to the real world can come in many ways. Classic processes in the bamboo and wood industries inspired the solution with chordal and radial knives in cutting GML_m^n surfaces and bodies. This is not surprising, since this real world, in particular botany, was also the source of inspiration for Gielis transformations [9]. As generalizations of Lamé curves, they turn out to be directly related to radial knives or drawing tools, and integrate seamlessly with GML_m^n bodies and surfaces. There are many connections to other fields of (differential) geometry, applied mathematics and science [10]).

Figure 13a shows a fibre bundle, and just as the Möbius band is a nontrival example of a fibre bundle, GML_m^n can be thought of as models for fibre bundles, which, when twisted and cut, become one sided. It does not take a big leap of imagination to extend the notion of strings with the mathematical methods developed for GML_m^n bodies and surfaces. Figure 13b shows a generalized cylinder, but now it is not directly connected, but via branes, very popular these days in physics. With the appropriate cutting tools and rules a GML_5^n wormhole becomes a single body one displaying the Möbius phenomenon.
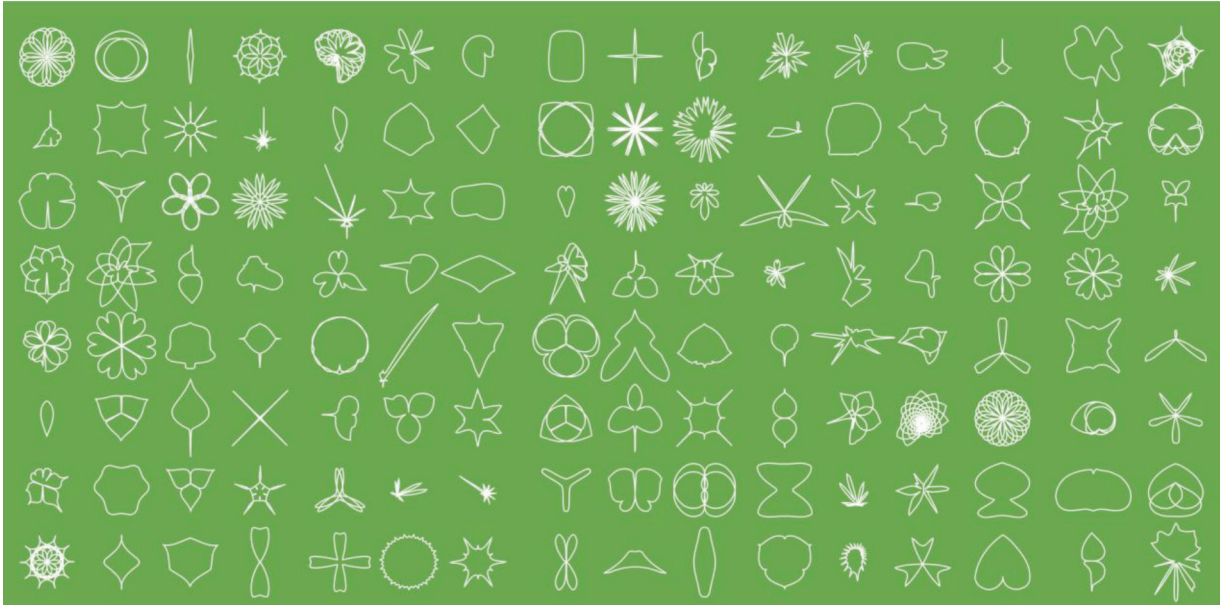
Figure 14 | Variational supercurves [18,19].

5.2. Gielis Transformations

The analytical representation of chordal and radial knives is directly related to classical trigonometric functions and the position vector. In this respect, Gielis transformations provide for a stretchable position vector [10]. In its original formulation it describes simple curves from $[0, 2\pi]$ for integer m and from $[0, k2\pi]$ for $m = p/q$ with p and q relative prime, but different sectors of a curve or disk with different parameters can be defined with the appropriate transition functions, resulting in variational supercurves (Figure 14). Further generalizations, retaining the Pythagorean compact structure, include the use of different functions instead of trigonometric functions in the denominator of Equation (4) [20].

One can also make any number of shapes with the following analytical representation [21].

$$\boldsymbol{r}_{i,j} = \hat{\boldsymbol{r}}_{i,j}\sqrt{x_{i,j}^2 + y_{i,j}^2}$$

$$x_{i,j} = A_{i,j}R_{i,j}(\theta_{i,j})\cos\theta_{i,j}$$

$$y_{i,j} = B_{i,j}R_{i,j}(\theta_{i,j})\sin\theta_{i,j}$$

$$R_{i,j}(\theta_{i,j}) = \left(\left| \frac{\cos(m_{i,2j-1}\theta_{i,j}/4)}{a_{i,2j-1}} \right|^{n_{i,2j-1}} + \left| \frac{\sin(m_{i,2j}\theta_{i,j}/4)}{a_{i,2j}} \right|^{n_{i,2j}} \right)^{-\frac{1}{b_{i,j}}}$$

where $\theta_{i,j} \in [-\pi, \pi]$ is the polar angle characterising the local coordinates system; $m_{i,2j-1}$, $m_{i,2j}$, $n_{i,2j-1}$, $n_{i,2j} \in \mathbb{R}^+$ (positive real numbers), $a_{i,2j-1}$, $a_{i,2j}$ and $b_{i,2j} \in \mathbb{R}_0^+$ (strictly positive real numbers), and $A_{i,j}$, $B_{i,j}$ are appropriate scaling factors; $i = 1, \dots p$ and $j = 1, \dots q$ and $M = p \cdot q$ being the total number of shapes. Additional rotation parameters can easily be introduced.

The unified geometrical description of GML surfaces and bodies and Gielis' transformations allows for the exact description of irregular shapes using an analytical formula and this translate into the possibility of building flexible tools to carry out sensitive analyses to geometrical parameter variations.

CONFLICTS OF INTEREST

The authors declare they have no conflicts of interest.

SUPPLEMENTARY MATERIALS

- Tables cutting GML_4 and GML_5.

- Videos of chordal and radial knives.

Supplementary data related to this article can be found at https://doi.org/10.2991/gaf.k.201210.001.

REFERENCES

[1] Tavkhelidze IN. About connection of the generalized Möbius-Listing's surfaces with sets of ribbon knots and links. In: Proceedings of Ukrainian Mathematical Congress. Kiev, Ukraine: S.2 Topology and Geometry; vol. 2, 2011, pp. 177–90.

[2] Tavkhelidze I, Caratelli D, Gielis J, Ricci PE, Rogava M, Transirico M. On a geometric model of bodies with "Complex" configuration and some movements. In: Modeling in Mathematics. Paris: Atlantis Press; 2017, pp. 129–58.

[3] Gielis J, Tavkhelidze I, Ricci PE. About "bulky" links generated by generalized Möbius–listing bodies GML_2^n. J Math Sci 2013;193; 449–60.

[4] Tavkhelidze I, Cassisa C, Gielis J, Ricci PE. About "Bulky" Links generated by Generalized Möbius-Listing bodies GML_3^n. Rend Lincei-Mate Appl 2013;24;11–38.

[5] Caratelli D, Gielis J, Ricci PE, Tavkhelidze I. Some properties of "bulky" links generated by generalized Möbius–Listing bodies GML_4^n. J Math Sci 2016;216;509–18.

[6] Tavkhelidze I, Ricci PE. Some properties of "bulky" links, generated by generalised Möbius–Listing's bodies GML_m^n {0}. In: Modeling in Mathematics. Paris: Atlantis Press; 2017, pp. 159–85.

[7] Pinelas S, Tavkhelidze I. Analytic representation of generalized Möbius-Listing's Bodies and classification of links appearing after their cut. In: International Conference on Differential & Difference Equations and Applications. Cham: Springer; 2017, pp. 477–93.

[8] Gielis J, Tavkhelidze I. The general case of cutting of GML surfaces and bodies. 2020;3;48.

[9] Gielis J. A generic geometric transformation that unifies a wide range of natural and abstract shapes. Am J Bot 2003;90;333–8.

[10] Gielis J. The geometrical beauty of plants. Paris: Atlantis Press; 2017, pp. 1–229.

[11] Tavkhelidze I, Gielis J. The process of cutting GML_n^m bodies with d_m-knives. In: Reports of the Enlarged Sessions of the Seminar of I. Tbilisi, Georgia: Vekua Institute of Applied Mathematics; vol. 32, 2018.

[12] Tavkhelidze I, Gielis J. d_m-knives and the process of cutting of GML_n^m bodies. In: Reports of the Enlarged Sessions of the Seminar of I. Tbilisi, Georgia: Vekua Institute of Applied Mathematics; vol. 33, 2019.

[13] Gielis J, Tavkhelidze I. The Möbius phenomenon in Generalized Möbius-Listing bodies with cross section of odd and even polygons. In: Report of the Enlarged Sessions of the Seminar of I. Tbilisi, Georgia: Vekua Institute of Applied Mathematics; vol. 34, 2020.

[14] Sloane NJA, Plouffe S. Number of intersections of diagonals in the interior of regular n-gon. The Encyclopedia of Integer Sequences. San Diego, USA: Academic Press; 1995.

[15] Buckberg GD. Basic science review: the helix and the heart. J Thorac Cardiovasc Surg 2002;124;863–83.

[16] Torrent-Guasp F, Buckberg GD, Clemente C, Cox JL, Coghlan HC, Gharib M. The structure and function of the helical heart and its buttress wrapping. I. The normal macroscopic structure of the heart. Semin Thorac Cardiovasc Surg 2001;13;301–19.

[17] Weeks J. The shape of space (Pure and Applied Mathematics), vol. 96. New York: Marcel Dekker, Inc.; 1987.

[18] Gielis J, Bastiaens E, Krikken T, Kiefer A, de Blochouse M. Variational Superformula curves for 2D and 3D graphic arts. In: ACM SIGGRAPH 2004 Posters. Association for Computing Machinery; 2004, p. 5.

[19] Gielis J, Bastiaens E, Beirinckx B. Computer Graphics Systems and Methods. U.S. Patent Application No. 10/870,683, International Publication Number WO 2004/111885, 2005.

[20] Gielis J, Natalini P, Ricci PE. A note about generalized forms of the Gielis formula. In: Modeling in Mathematics. Paris: Atlantis Press; 2017, pp. 107–16.

[21] Mescia L, Chiapperino MA, Bia P, Lamacchia CM, Gielis J, Caratelli D. Design of electroporation process in irregularly shaped multicellular systems. Electronics 2019;8;37.